Minimization of the Renyi entropy production in the stationary states of the Brownian process with matched death and birth rates

Olgierd Cybulski and Volodymyr Babin
Institute of Physical Chemistry, Polish Academy of Sciences, Kasprzaka 44/52, 01-224 Warsaw, Poland

Robert Hołyst
Institute of Physical Chemistry, Polish Academy of Sciences, Kasprzaka 44/52, 01-224 Warsaw, Poland
and Department of Mathematics and Natural Sciences – College of Science, Cardinal Stefan Wyszyński University, Dewajtis 5, 01-815 Warsaw, Poland

(Received 29 May 2003; revised manuscript received 9 September 2003; published 28 January 2004)

We analyze the Fleming-Viot process. The system is confined in a box, whose boundaries act as a sink of Brownian particles. The death rate at the boundaries is matched by the branching (birth) rate in the system and thus the number of particles is kept constant. We show that such a process is described by the Renyi entropy whose production is minimized in the stationary state. The entropy production in this process is a monotonically decreasing function of time irrespective of the initial conditions. The first Laplacian eigenvalue is shown to be equal to the Renyi entropy production in the stationary state. As an example we simulate the process in a two-dimensional box.

DOI: 10.1103/PhysRevE.69.016110 PACS number(s): 05.70.Ln, 65.40.Gr, 05.90.+m

I. INTRODUCTION

Irreversible entropy production is one of the key quantities in nonequilibrium thermodynamics [1,2]. For open systems not far from the equilibrium states it has been conjectured by Prigogine that a system in the stationary states, compatible with the external constraints, adopts such configurations which minimize the entropy production (MEP). Far from equilibrium MEP breaks down, although part of the entropy production given by the contraction of the phase space has been shown to be minimized in some special cases [3]. In general one of the approaches to nonequilibrium statistical mechanics is related to the study of the entropy production and escape rate of transport processes far from equilibrium [4–7] with the emphasis on the Lyapunov exponents and the onset of chaos.

There is yet another approach to nonequilibrium systems from the perspective of nonextensive thermodynamics [8]. The construction of the nonextensive thermodynamics is based on the Tsallis or Renyi entropies. In both cases the entropy is the property of the whole system and cannot be defined for any subsystem. However, the Tsallis entropy is nonextensive in the strong sense; i.e., for two independent systems (independent in terms of the probabilities of configurations) the entropy of the sum of the systems is not equal to the sum of their entropies. The formalism of the nonextensive thermodynamics has been applied, e.g., to the onset of chaos in the logistic maps [9], anomalous diffusion in the presence of external forces [10], dynamic linear response in nonextensive systems [11], connection between self-organized critical dissipative systems and the Tsallis entropy [12,13], fractional diffusion process [14], and low-dimensional dissipative systems [15]. One of the goals of many papers devoted to the nonextensive thermodynamics was to analyze the formal structure of the theory and show which of the results of the theory for ordinary thermodynamics can be translated into the structure of nonextensive thermodynamics [8,16–19].

It is the purpose of this work to simulate a stochastic model of Brownian particles with death and branching (birth), which in the stationary state adopts such a configuration which minimizes the Renyi entropy production. This result is complementary to previous approaches, where the nonlinear Fokker-Planck equation (NLFPE) was studied for various thermostatics and the NLFPE was derived from maximization of the appropriate entropy functional [20,21].

Our methodology is as follows. We first define a nonlinear equation for the evolution of the probability density in which nonlinearity appears in integral form. From the form of the equation we deduce the form of the appropriate entropy as a functional of the probability distribution, $S[p]$. The entropy is chosen in such way that its evolution in time follows a prescription known from ordinary nonequilibrium thermodynamics—i.e.,

$$\frac{dS[p]}{dt} = -\lambda[p] + \sigma[p], \tag{1}$$

where λ is the flux of the entropy and σ is its production which must be positive definite. Moreover, we also insist that the entropy production σ must be minimized in the stationary state; i.e., the equation

$$\frac{\delta\sigma[p]}{\delta p} = 0 \tag{2}$$

must lead to a stationary distribution of p. Such a prescription for the entropy functional led us unambiguously to the Renyi entropy in the case of our process (described below):

$$S[p]=\frac{1}{1-\alpha}\ln\int p^{\alpha}, \tag{3}$$

with $\alpha=2$, where the integral is over the whole system.

The process, described by the aforementioned equations, which we study in this paper is the Brownian motion of a multiparticle system in a box with absorbing boundary conditions [22,23]. Additionally we assume that if one particle is killed at the boundary, another one, picked at random in the system, is duplicated, giving birth to a new particle in the same site. As we can see the birth rules are chosen in such a way as to keep the number of particles constant at each time step. Moreover, the nonextensive nature of the system is evident: the flux of the particles at the boundary affects immediately the distribution of the particles inside the system, no matter how large the system is. Such a system cannot be divided into subsystems.

The paper is organized as follows: In Sec. II we describe the system containing a finite number of Flemming-Viot particles. In Sec. III we introduce the continuous model of the above system, and we analyze the evolution of the probability distribution. In Sec. IV related thermodynamic functionals are studied, especially the entropy production. In Sec. V we present the results of a computer simulation of the two-dimensional systems. The Appendix contains the proofs of the H theorem equivalent for the entropy production.

II. BROWNIAN MOTION WITH MATCHED DEATH AND BIRTH RATES

Let us consider a system containing many particles each performing an independent random walk inside a given region. A special kind of boundary condition is imposed: a particle must vanish after reaching the border of the region, and, exactly at the same time, another particle (chosen at random) is duplicated. In other words, a particle is removed when it reaches any point located at the boundary. Simultaneously, a new particle is introduced and placed at the position of randomly chosen particle. It follows that the total number of the particles in the system is conserved. The probability of the multiplication process described above is identical for each particle. Further Brownian motions of the chosen particle, and its copy, are independent.

The evolution of the system under consideration depends on the number and initial position of the particles. Unfortunately, a quantitative description of the values characterizing the system state (like entropy or even the local density of particles) is burdened with fluctuations. Their significance vanishes in the limit when the number of particles goes to infinity.

Although we have performed numerical simulations of the aforementioned system with finite particle number, we do not include these results in the paper. Instead of that we examined the continuous model of probability distribution evolution. Both models—the many-particle and the continuous one (described in the following section)—give the same results in the limit of a large number of particles.

We will show that irrespective of the initial conditions, the particle distribution evolves towards a steady state. If the region has a connected interior, there exists exactly one steady state. Contrary to the system with reflective boundary conditions, the particle distribution in the steady state of the system under consideration is not uniform. Due to the absorbing boundary conditions, the particles tend to group in the inner part of the region rather than near the boundaries.

III. CONTINUOUS MODEL

The probability density function (PDF) of the system, $p(\mathbf{r},t)$, satisfies the following equations [22]:

$$\frac{\partial}{\partial t}p(\mathbf{r},t)=K\Delta p(\mathbf{r},t)+\Lambda(t)p(\mathbf{r},t), \tag{4}$$

$$\int_V p(\mathbf{r},t)\mathrm{d}V=1, \tag{5}$$

where K is a positive diffusion constant, and the integration is over whole volume of the system. The term $\Lambda(t)p(\mathbf{r},t)$ represents particle multiplication at the point $\mathbf{r}$ at time t. A function $\Lambda(t)$ is chosen to compensate the actual absorption of particles at the boundaries. For each point $\mathbf{r}_0$ at the boundary of the region, the following boundary condition is imposed:

$$p(\mathbf{r_0},t)=0. \tag{6}$$

Combining Eq. (4) with the condition given by Eq. (6) implies that

$$\Delta p(\mathbf{r_0},t)=0 \tag{7}$$

for each $\mathbf{r}_0$ on the boundary.

Integrating Eq. (4) over the system, we obtain

$$\Lambda(t)=-K\int_V \Delta p\mathrm{d}V \tag{8}$$

or, applying the Green theorem,

$$\Lambda(t)=-K\oint_{\partial V}\boldsymbol{\nabla}p\cdot\mathrm{d}\mathbf{S}. \tag{9}$$

By substituting $\Lambda(t)$ we can rewrite Eq. (4) governing the evolution of the system in the following form:

$$\frac{\partial p}{\partial t}=K\Delta p-K\left(\int_V \Delta p\mathrm{d}V\right)p. \tag{10}$$

By setting $\partial p/\partial t=0$, we obtain the equation for the stationary solution $p_s(\mathbf{r})$:

$$\Delta p_s(\mathbf{r})=\left(\int_{V'}\Delta p_s(\mathbf{r}')\mathrm{d}V'\right)p_s(\mathbf{r}). \tag{11}$$

The equation must be satisfied for each $\mathbf{r}$. However, the expression in brackets is a number independent of $\mathbf{r}$. Therefore Eq. (11) is the equation for the Dirichlet Laplacian eigenfunctions for the considered region [24,25]. Only one of such

eigenfunctions satisfies the condition of non-negative PDF values. It is the eigenfunction associated with the first eigenvalue λ_1 (with the notion as in the next paragraph):

$$\Delta p_s = \lambda_1 p_s . \tag{12}$$

This stationary solution is always asymptotically achieved in the limit of $t \to \infty$ (proved in [25]).

A. Evolution in the reciprocal space

The form of the stationary state suggests the eigenfunction decomposition to be a helpful tool also in analysis of dynamics far from the stationary state. As long as the region is limited, the Dirichlet Laplacian eigenfunctions and eigenvalues form a countable system [24,25]. All the eigenvalues are negative [25]. Regardless of the dimension of space, we can enumerate the eigenfunctions and eigenvalues with an index $i = 1,2,\ldots,+\infty$ in such a way that the eigenvalues form the ordered sequence

$$0 > \lambda_1 > \lambda_2 \geqslant \lambda_3 \geqslant \lambda_4 \geqslant \cdots - \infty . \tag{13}$$

If the region has a connected interior, the first eigenvalue λ_1 cannot be degenerated [25]. However, further eigenvalues may be degenerated.

Let us consider the span of the orthonormal system of Dirichlet Laplacian eigenfunctions $u_i(\mathbf{r})$ corresponding to the eigenvalues λ_i and the sequence of real numbers β_i with definitions as follows:

$$\Delta u_i(\mathbf{r}) = \lambda_i u_i(\mathbf{r}) \qquad \int_V u_i(\mathbf{r}) \mathrm{d}V = \beta_i , \tag{14}$$

$$\int_V u_i(\mathbf{r}) u_j(\mathbf{r}) \mathrm{d}V = \begin{cases} 0 & \text{if } i \neq j, \\ 1 & \text{if } i = j. \end{cases} \tag{15}$$

In such a basis we expand the time-dependent PDF:

$$p(\mathbf{r},t) = \sum_{i=1}^{\infty} c_i(t) u_i(\mathbf{r}), \tag{16}$$

The real coefficients c_i are chosen in such a way to guarantee non-negative values of the PDF inside the region and to provide the normalization

$$\int_V p(\mathbf{r},t) \mathrm{d}V = \sum_{i=1}^{\infty} c_i(t) \beta_i = 1. \tag{17}$$

In further consideration we will use the fact that at each moment $c_1 \neq 0$. To prove it, let us suppose that $c_1 = 0$. From Eq. (15) we would obtain

$$c_1 = 0 \;\Rightarrow\; \int_V u_1(\mathbf{r}) p(\mathbf{r},t) \mathrm{d}V = 0. \tag{18}$$

The first eigenfunction $u_1(\mathbf{r})$ does not change sign inside the region [24,25]. Moreover, if the region has a connected interior, $u_1(\mathbf{r}) \neq 0$ for each $\mathbf{r}$ in the interior of the region. To reconcile this with Eqs. (17) and (18), the PDF would have to change sign in the region. Because the PDF must be non-negative, we must have $c_1 \neq 0$.

Henceforth, if not otherwise noted, all summations run from 1 to $+\infty$.

Equation (10), when combined with Eq. (16), takes the following form:

$$\frac{1}{K} \sum_i \frac{\mathrm{d}c_i}{\mathrm{d}t} u_i = \sum_i c_i \lambda_i u_i - \sum_i c_i u_i \sum_j c_j \lambda_j \beta_j . \tag{19}$$

Thus the expansion coefficients $c_i(t)$ satisfy ordinary differential equations of the form

$$\frac{1}{K} \frac{\mathrm{d}c_i}{\mathrm{d}t} = \lambda_i c_i - c_i \sum_j \beta_j c_j \lambda_j . \tag{20}$$

Depending on the actual configuration, the absolute values $\|c_i\|$ may decrease as well as increase at the given moment. However, except for $\|c_1\|$, they approach 0 in the last stage of evolution [see the note below Eq. (12)].

B. Asymptotic behavior

The stationary solution, given by Eq. (12), has the form

$$p_s(\mathbf{r}) = c_1 u_1(\mathbf{r}), \tag{21}$$

where $c_1 = 1/\beta_1$. In the long-time limit, the PDF becomes equal to this stationary solution, with some small addition of higher eigenfunctions. Near the stationary state Eq. (20) becomes linear; thus for $i \geqslant 2$ the coefficients c_i vanish exponentially, with the decay rate equal to $K(\lambda_1 - \lambda_i)$.

Let us consider the competition of two different coefficients $c_i \neq 0$ and $c_j \neq 0$. If $\lambda_i > \lambda_j$, then there will be a time when (and after which) $|c_i| \gg |c_j|$, regardless of the initial values. For this reason, in the last stage of reaching the stationary state only the eigenfunctions associated with the lowest possible eigenvalues (as far as modulus is concerned) are present in the PDF. The first of these eigenvalues is always λ_1, but the next relevant—say, λ_q—may be higher than λ_2. That is because selective excitations are possible (some coefficients may be exactly zero, e.g., if the initial state has the same symmetry as the stationary state). Moreover, the eigenvalue λ_q may be degenerated. Thus in the general case the long-time limit of PDF is assumed in the following form:

$$p(\mathbf{r}, t \to \infty) \approx c_1(t) u_1(\mathbf{r}) + \sum_{q'} c_{q'}(t) u_{q'}(\mathbf{r}), \tag{22}$$

where q' runs over the orthogonal eigenfunctions associated with λ_q (first excited eigenvalue, usually $q = 2$). From Eq. (20) we obtain

$$\frac{\mathrm{d}c_1}{\mathrm{d}t} = c_1 K(\lambda_1 - \lambda_q) \sum_{q'} \beta_{q'} c_{q'} , \tag{23}$$

$$\frac{\mathrm{d}c_{q'}}{\mathrm{d}t} = c_{q'} K(\lambda_q - \lambda_1) c_1 \beta_1 \quad (\text{for each } q'). \tag{24}$$

We assume that $c_{q'}$ are small and $c_1\beta_1 \approx 1$. It allows us to linearize the above equations,

$$\frac{\mathrm{d}c_1}{\mathrm{d}t} = \frac{K}{\beta_1}(\lambda_1 - \lambda_q)\sum_{q'} \beta_{q'} c_{q'}, \tag{25}$$

$$\frac{\mathrm{d}c_{q'}}{\mathrm{d}t} = c_{q'} K(\lambda_q - \lambda_1) \quad (\text{for each } q'), \tag{26}$$

and to find the solutions consistent with previous assumptions:

$$c_{q'} \approx A_{q'} e^{K(\lambda_q - \lambda_1)t} \quad (\text{for each } q'), \tag{27}$$

$$c_1 \approx \frac{1}{\beta_1} - \frac{1}{\beta_1}\left(\sum_{q'} \beta_{q'} A_{q'}\right) e^{K(\lambda_q - \lambda_1)t}. \tag{28}$$

As we can see, the relaxation towards a steady state is exponential. Notice that the assumption $A_{q'} \neq 0$ is insufficient to ensure a nonzero value of $\mathrm{d}c_1/\mathrm{d}t$ in Eq. (25), because the factors $\beta_{q'}$ may be zero for $q' \geqslant 2$ or the sum of $\beta_{q'} A_{q'}$ may vanish for some $A_{q'}$ combinations.

IV. ENTROPY AND ITS PRODUCTION

According to the discussion presented in the Introduction, we have found that Eq. (3) with $\alpha = 2$, i.e.,

$$S[p] = -\ln\left(V \int_V p^2 \mathrm{d}V\right), \tag{29}$$

describes the entropy of the system. Additionally, the volume of the region, V, has been added in Eq. (29) for dimensional reasons.

This entropy describes the system only, and it does not account for any changes in the environment. If we want the considered system to be physical, we must treat the death and birth as external processes. Something takes all the particles from the boundaries and moves them back to the interior of the region. The entropy of that external pumping device must increase, as in the case of the entropy of the Maxwell's daemon. That is a reason why the entropy (29) may decrease as well as increase during the evolution. Using Eq. (4) we obtain the equation for the evolution of S:

$$\frac{\mathrm{d}S}{\mathrm{d}t} = \frac{-2K\int_V p\Delta p \mathrm{d}V}{\int_V p^2 \mathrm{d}V} - 2\Lambda(t). \tag{30}$$

On the right side we can see the sum of two terms, which could be interpreted as the entropy production and the entropy flux. By using formula (9) we get it in a more explicit form:

$$\frac{\mathrm{d}S}{\mathrm{d}t} = \underbrace{\frac{-2K\int_V p\Delta p \mathrm{d}V}{\int_V p^2 \mathrm{d}V}}_{\text{entropy production},\,\sigma} + \underbrace{2K \oint_{\partial V} \nabla p \cdot \mathrm{d}\mathbf{S}}_{\text{outgoing flux}} \tag{31}$$

Due to the non-negativity of the PDF, the outgoing entropy flux must be negative or zero.

However, the entropy production $\sigma[p]$ is always positive. It results from the condition (6) and the Green theorem:

$$\sigma[p] = \frac{-2K\int_V p\Delta p \mathrm{d}V}{\int_V p^2 \mathrm{d}V} = \frac{2K\int_V (\nabla p)^2 \mathrm{d}V}{\int_V p^2 \mathrm{d}V}. \tag{32}$$

In the reciprocal space, with definitions given by Eqs. (14) and (16), the entropy production takes the form

$$\sigma[p] = \frac{-2K\sum_i c_i^2 \lambda_i}{\sum_i c_i^2}. \tag{33}$$

Since $\lambda_1 < 0$ and $\|\lambda_i\| > \|\lambda_1\|$ for each $i > 1$, the entropy production is minimized in the stationary state:

$$\sigma_{\min} = \sigma_s = -2K\lambda_1. \tag{34}$$

Moreover, beyond the stationary state the following relation (proved in the Appendix) is always satisfied:

$$\frac{\mathrm{d}\sigma}{\mathrm{d}t} < 0; \tag{35}$$

i.e., σ is a monotonically decreasing function of time. This is an equivalence of the H theorem for the entropy production in the irreversible nonextensive system.

Asymptotic behavior

Using the asymptotic PDF expansion from Eq. (22) we obtain

$$\begin{aligned}\sigma &\approx -2K\frac{c_1^2\lambda_1 + \lambda_q\sum c_{q'}^2}{c_1^2 + \sum c_{q'}^2} \\ &= -2K\left[\lambda_1 + (\lambda_q - \lambda_1)\frac{\sum c_{q'}^2}{c_1^2} + O\left(\left(\frac{\sum c_{q'}^2}{c_1^2}\right)^2\right)\right].\end{aligned} \tag{36}$$

Substituting c_1 and $c_{q'}$ by Eqs. (27) and (28) and neglecting higher-order terms we obtain

$$\sigma \approx -2K\left[\lambda_1+(\lambda_q-\lambda_1)\beta_1^2\left(\sum A_{q'}^2\right)e^{2K(\lambda_q-\lambda_1)t}\right]$$
$$=\sigma_s+\|\text{const}_1\|\times e^{2K(\lambda_q-\lambda_1)t}, \tag{37}$$

where σ_s means entropy production in the stationary state.

Similarly we calculate asymptotic form of the entropy time derivative:

$$\frac{dS}{dt}=-2\frac{c_1\dot{c}_1+\sum c_{q'}\dot{c}_{q'}}{c_1^2+\sum c_{q'}^2}. \tag{38}$$

We consider two separate cases (see the notice at the end of Sec. III), depending on the value of $\dot{c}_1$ given by Eq. (23).

(i) If $\dot{c}_1=0$, the leading time-dependent term in expansion of Eq. (38) is a quadratic function of the perturbation amplitudes $A_{q'}$:

$$\frac{dS}{dt}=\|\text{const}_1\|\times e^{2K(\lambda_q-\lambda_1)t}, \tag{39}$$

where const_1 is the same as in Eq. (37).

(ii) If $\dot{c}_1\neq 0$, the leading term is a linear function of a perturbation amplitudes $A_{q'}$:

$$\frac{dS}{dt}=\text{const}_2\times e^{K(\lambda_q-\lambda_1)t}, \tag{40}$$

where

$$\text{const}_2=2K(\lambda_q-\lambda_1)\sum_{q'}\beta_{q'}A_{q'}.$$

In both cases the long-time approach of the entropy function to the stationary state is exponential. The perturbations being orthogonal with respect to the stationary state [case (i)] give the asymptotic increasing of the entropy with the same exponent as in the relaxation of entropy production [compare Eq. (39) for entropy and Eq. (37) for production].

All the other perturbations give the entropy relaxation conforming to Eq. (40), with the exponent twice smaller than in the entropy production relaxation, Eq. (37). The direction of long-time entropy approach to the stationary state may be increasing as well as decreasing in this case.

V. 2D SIMULATIONS

A. Simulation method

We solve Eq. (10) in the discrete space with time step $\Delta t=1$, lattice units $\Delta x=\Delta y=1$, and discrete Laplacian $\Delta p(x,y)$ defined as follows:

$$\Delta_{i,j}^t=p_{i-1,j}^t+p_{i+1,j}^t+p_{i,j-1}^t+p_{i,j+1}^t-4p_{i,j}^t. \tag{41}$$

Applying the Euler method to Eq. (10) we obtain

$$p_{i,j}^{t+1}-p_{i,j}^t=K\Delta_{i,j}^t-Kp_{i,j}^t\sum_{n,m}\Delta_{n,m}^t. \tag{42}$$

Unfortunately, that differential scheme is not time centered. Consequently, it may lead to the accumulation of numerical errors, especially to the loss of PDF normalization. To avoid this, one may use the modified Euler method or the Runge-Kutta algorithm.

Instead of that, we consider a small modification of the aforementioned scheme:

$$p_{i,j}^{t+1}-p_{i,j}^t=K\Delta_{i,j}^t-Kp_{i,j}^{t+1}\sum_{n,m}\Delta_{n,m}^t. \tag{43}$$

Now the normalization of the PDF is preserved as long as the calculations are exact. From Eq. (43) we obtain

$$p_{i,j}^{t+1}=\frac{p_{i,j}^t+K\Delta_{i,j}^t}{1+K\sum_{n,m}\Delta_{n,m}^t}. \tag{44}$$

By the summation over i,j we get

$$\sum_{i,j}p_{i,j}^t=1\Rightarrow\sum_{i,j}p_{i,j}^{t+1}=1. \tag{45}$$

It is not sufficient to guarantee conservation of the normalization in numerical calculations. Numerical inexactness may accumulate during successive iterations of Eq. (44). Let us suppose that the PDF is normalized to $1+\epsilon$, where ϵ is a small number of any sign:

$$\sum_{i,j}p_{i,j}^t=1+\epsilon_t. \tag{46}$$

From Eq. (44) we obtain

$$\epsilon_{t+1}=\frac{1}{1+K\sum_{n,m}\Delta_{n,m}^t}\epsilon_t. \tag{47}$$

The sum in the denominator is negative; thus the error amplification factor is greater than unity.

To avoid this (i.e., to stabilize the method) we rewrite Eq. (44) in the following form:

$$p_{i,j}^{t+1}=\frac{p_{i,j}^t+K\Delta_{i,j}^t}{\sum_{n,m}(p_{n,m}^t+K\Delta_{n,m}^t)}. \tag{48}$$

Now the normalization of the PDF is restored in each iteration.

For practical reasons the numerical calculations are performed in two steps. In the first step, the auxiliary matrix elements $q_{i,j}$ are calculated:

$$q_{i,j}=p_{i,j}^t+K\Delta_{i,j}^t. \tag{49}$$

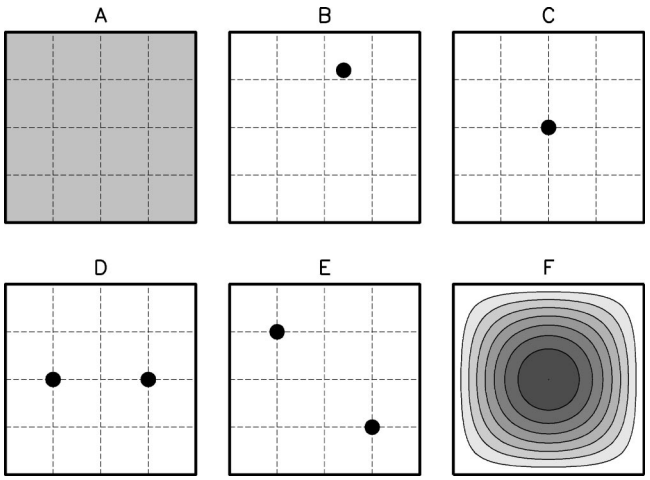

FIG. 1. Various initial states (A uniform, B, C, D, E localized at points) and the contour plot of the stationary state (F) of the PDF within a two-dimensional square region of size 100×100.

This step represents pure diffusion.

In the second step the normalization is restored:

$$W=\left(\sum_{i,j} q_{i,j}\right)^{-1}, \quad p_{i,j}^{t+1}=Wq_{i,j}. \tag{50}$$

As we can see, our simulation method may be treated as interleaving diffusion and renormalization steps.

B. Square region

The evolution of the PDF within the square region is analyzed. The lattice used in the computer simulation has 101×101 nodes, which corresponds to the square of 100×100 lattice units.

The initial conditions used and the stationary state of the PDF are shown in Fig. 1. The simulation results are in accordance with the theoretical considerations. Regardless of the initial conditions, the PDF of the stationary state obtained from the simulation is approximately equal to the corresponding stationary state of the continuous system:

$$p_s(\mathbf{r})=\frac{2}{\sqrt{N_xN_y}}\sin\frac{\pi x}{N_x}\sin\frac{\pi y}{N_y}. \tag{51}$$

In the case of the initial conditions A (Fig. 1) the entropy production is always smaller than outgoing entropy flux [defined in Eq. (31)]; thus the entropy of the system decreases with time. In cases B, C and D this relation is inverted. Case E is more interesting (see Fig. 2): at the beginning the production is greater than the flux, but it becomes smaller after 3265 simulation steps (with $K=1/8$).

The asymptotic behavior of $\mathrm{d}S/\mathrm{d}t$ is studied for each of the initial conditions from Fig. 1. As we can see in Fig. 3, the relaxation of $|\mathrm{d}S/\mathrm{d}t|$ near the stationary state (after long evolution time) is exponential; however, the exponent value depends on the initial conditions.

The asymptotes are fitted to the tails of the curves from Fig. 3 by linear regression:

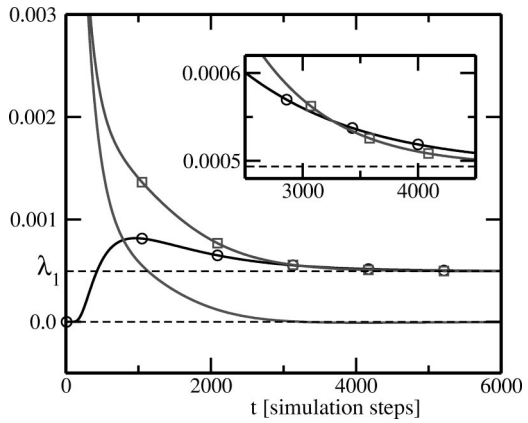

FIG. 2. The entropy production σ (squares), the escape flux 2Λ (circles), and the entropy time derivative (no symbols) of the system started from initial condition E, Fig. 1. In magnified scale (inset) we can see the crossing of curves, after which $\mathrm{d}S/\mathrm{d}t$ becomes negative, and further it approaches zero from below.

$$\ln\left|\frac{\mathrm{d}S}{\mathrm{d}t}\right|\approx\tilde{a}t+\tilde{b}. \tag{52}$$

From Eqs. (39) and (40) we obtain

$$\tilde{a}=\xi_qK(\lambda_q-\lambda_1), \quad \text{where} \quad \xi_q=\{1 \text{ or } 2\}. \tag{53}$$

For the square, with $N_x=N_y=N$, we obtain (with accuracy limited by the discretization error)

$$\tilde{a}\approx-\xi_{m,n}\frac{K\pi^2}{N^2}(m^2+n^2-2), \tag{54}$$

where $m\geqslant1$ and $n\geqslant1$ denote the leading eigenvalue $\lambda_{m,n}$, and $\xi_{m,n}$ can be written as

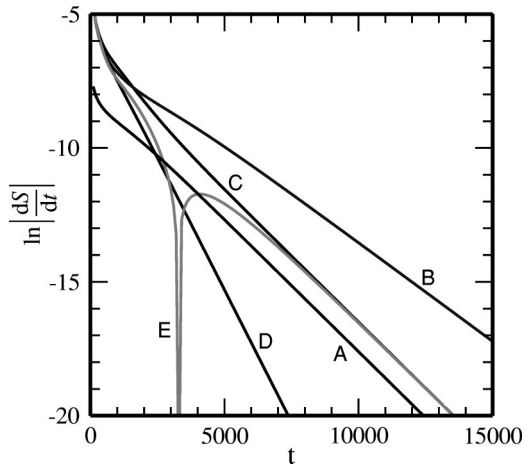

FIG. 3. Long-time behavior of $\ln|\mathrm{d}S/\mathrm{d}t|$ for the initial conditions as in Fig. 1 (with consistency of the letter signs). These curves have linear asymptotes with three different slopes. Note that curve E has the singularity (when the logarithm argument passes through 0), and further it runs along curve C.

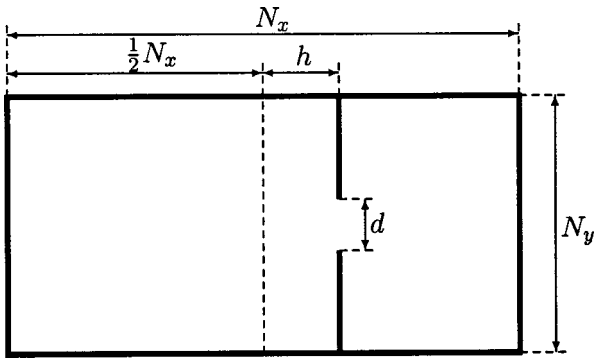

FIG. 4. The rectangular region divided into two segments: h, offset of the wall position related to the middle of the rectangle; d, size of the hole between segments.

$$\xi_{m,n}=2-\frac{[(-1)^m-1][(-1)^n-1]}{4}. \tag{55}$$

In order to assign the asymptotes to the appropriate eigenvalues we test the expression

$$M=\frac{-\tilde{a}N^2}{K\pi^2}, \tag{56}$$

which should be a positive integer number:

$$M=\xi_{m,n}(m^2+n^2-2). \tag{57}$$

With an accuracy better than 10^{-3} we get the values $M=8$ (case A), $M=6$ (B), $M=8$ (C), $M=16$ (D), and $M=8$ (E). It leads to the following identification of eigenvalues:

$\lambda_{1,2}$ or $\lambda_{2,1}$ (case B),
$\lambda_{1,3}$ or $\lambda_{1,3}$ (cases A,C,E),
$\lambda_{3,3}$ (case D).

Asymptotic behavior similar to case B will occur most often after applying random or any asymmetric initial conditions.

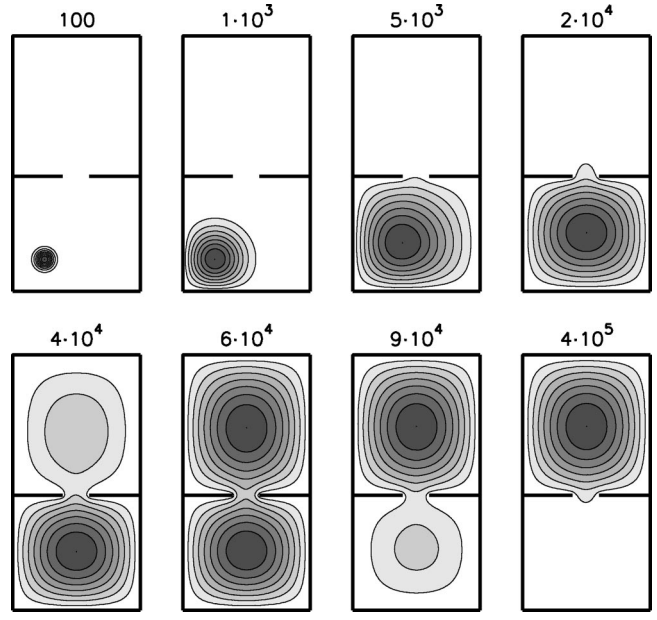

FIG. 5. Contour plot snapshots of PDF evolution (details in the text). The numbers denote a time from the beginning of the simulation (measured in simulation steps). The time intervals between subsequent snapshot are changing—the evolution runs fast at the beginning and much slower during the flow between chambers.

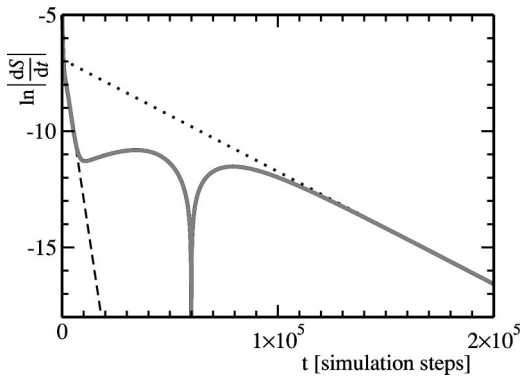

FIG. 6. $\ln|dS/dt|$ as a function of time in the system shown in Fig. 5. Two characteristic exponents are observed: for the rapid process of entropy relaxation in a single chamber (dashed line) and for the slow transport between chambers [dotted line; see Eqs. (52) and (60)].

C. Transfer between two chambers

We investigate the evolution of the PDF in the two-dimensional, rectangular region divided by the wall into two chambers (see Fig. 4). The wall is placed across the rectangle with the shift h, and in the middle it has a hole of size d.

The lattice used in the simulation has 201×101 nodes ($N_x=200$, $N_y=100$). Figure 5 shows snapshots of the PDF evolution for parameter values $d=20$, $h=-10$ (measured in lattice units). The initial condition is $p_{25,25}=1$ (the center point of the left, bottom quarter of the smaller chamber) and $p_{i,j}=0$ for the rest of the nodes.

The two stages of evolution can be identified here. The first stage is fast—the PDF covers the smaller chamber, taking a form similar to the stationary state of the single square

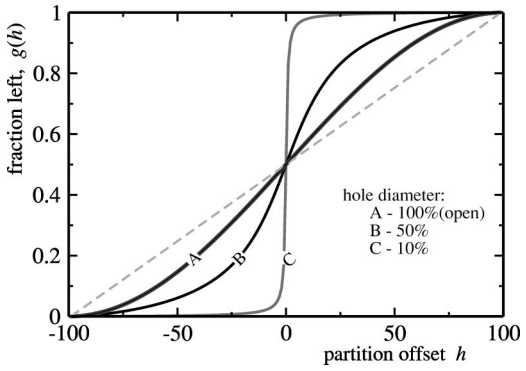

FIG. 7. The fraction of particles left in the first chamber as a function of the dividing wall position h. Curve A is a shifted sine [see $g_{\text{open}}(h)$ in the text]. Curve C runs near the step function $g_{\text{closed}}(h)$ (not shown here). The dashed line $g_{\text{ref}}(h)$, is for the system with reflecting boundary conditions.

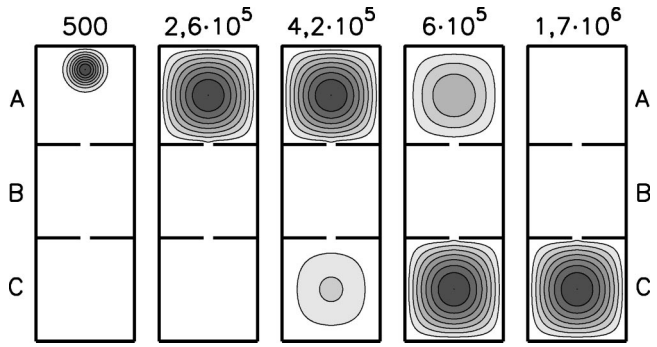

FIG. 8. Contour plot snapshots of PDF evolution in the rectangular region divided on three unequal chambers: A, 100×100; B, 100×95; and C, 100×105 lattice units. The numbers above the plots denote a time from the beginning of the simulation (measured in simulation steps).

region. In the second, much slower stage, the PDF is pouring from the smaller chamber into the greater one. During this flow the PDF in each chamber lies similarly to the stationary state of closed chamber (with no hole). In this sense the evolution of the system could be considered as the sequence of quasistationary states of two subsystems.

The changes of the $\ln|dS/dt|$ in time are shown in Fig. 6. The sloping segments of this curve allow one to find exponents characterizing the processes described above. The same exponents could be evaluated approximately using perturbation theory. In the limit when the hole diameter d becomes small (but still for $h\neq 0$), the lowest Laplacian eigenvalues approach the eigenvalues of the separate chambers:

$$\lambda_- = -\pi^2\left(\frac{1}{N_y^2}+\frac{1}{(N_x/2-h)^2}\right), \tag{58}$$

$$\lambda_+ = -\pi^2\left(\frac{1}{N_y^2}+\frac{1}{(N_x/2+h)^2}\right), \tag{59}$$

where λ_+ corresponds to the smaller chamber if $h<0$, as in the example under consideration. In this approximation the

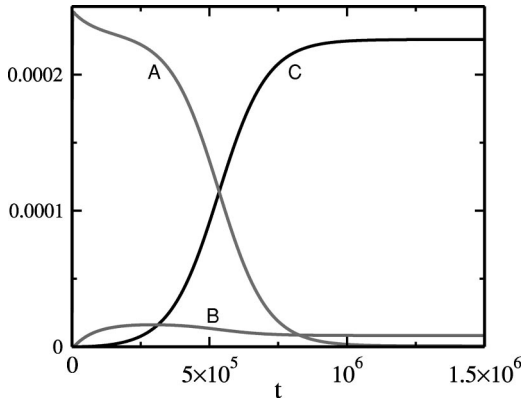

FIG. 9. Values of the PDF in the middle of each chamber in the system shown in Fig. 8.

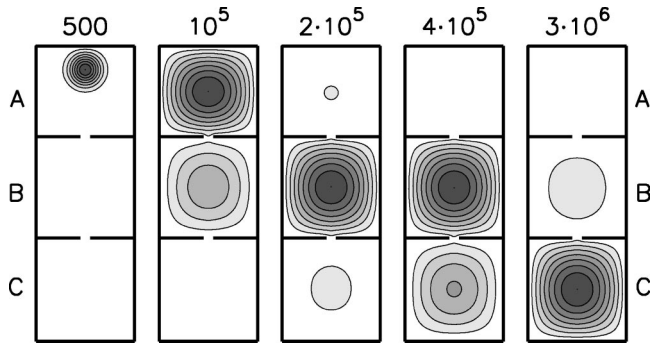

FIG. 10. The same as in Fig. 8, but with different chamber sizes: A, 100×92; B, 100×103; and C, 100×105 lattice units.

slope of the asymptote [defined in Eq. (52)] for the slow process (i.e., the transfer of particles between chambers) has the form

$$\tilde{a} = K(\lambda_- - \lambda_+). \tag{60}$$

In the case presented in Fig. 6 the fitted $\tilde{a}$ value differs from the aforementioned approximation by less than 4%.

D. Stationary state as a function of parameters

Let us consider the following function of parameters h and d (see Fig. 4) defined in the stationary state:

$$g(h,d) = \int_0^{N_y}\int_0^{N_x-h} p_s(\mathbf{r})\,dx\,dy. \tag{61}$$

It describes the fraction of particles localized in the first chamber.

In the case of $d=N_y$ (rectangular region without an inner wall) the function $g(h)$ is sinusoidal:

$$g_{\text{open}}(h) = g(h,N_y) = \frac{1}{2}+\frac{1}{2}\sin\left(\frac{h\pi}{N_x}\right). \tag{62}$$

When $d\to 0$ (fully separated chambers; due to connectivity loss, we consider this case only in the limit with $d\to 0^+$) we obtain the step function

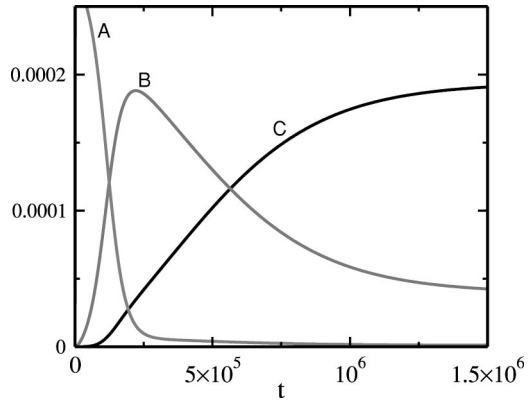

FIG. 11. Values of the PDF in the middle of each chamber in the system shown in Fig. 10.

$$g_{\text{closed}}(h)=g(h,d\to 0^{+})=\begin{cases}0 & \text{if } h<0,\\ 1/2 & \text{if } h=0,\\ 1 & \text{if } h>0.\end{cases} \tag{63}$$

Figure 7 shows these extreme curves and some intermediate ones.

For comparison, an analogous curve is shown for the system with reflective boundaries. It is a linear function of h:

$$g_{\text{ref}}(h)=\frac{1}{2}+\frac{h}{N_x}. \tag{64}$$

E. Transfer between three chambers

Two interesting examples of PDF evolution are studied in the system containing three chambers in series connection. The chambers are separated by walls with centered holes. Both systems are simulated on 301×101 lattices, and both are divided on three chambers by two walls. In the center of each wall there is a hole of size of 8 lattice units.

The chamber lengths are 100,95,105 in the first case (shown in Figs. 8 and 9) and 92,103,105 in the second case (Figs. 10 and 11). The initial conditions in both cases are the same: the whole PDF is localized at a single point of the first chamber (signed by letter A). Figures 8 and 10 show snapshots of the PDF contour plot during evolution. Figures 9 and 11 show the evolution of the local PDF value in the middle of each chamber, respectively.

VI. CONCLUSIONS

We have simulated a model system of Brownian particles in a box with absorbing boundary conditions, with a birth rate inside a system matching the death rate at the boundary. Such system satisfies a set of equations [Eqs. (1), (2), and (29)] for the Renyi entropy.

The distribution of Brownian particles in the stationary state minimizes the Renyi entropy production [Eqs. (33) and 34)].

If the evolution takes place in the set of regions connected by narrow channels, the final distribution is always centered in the middle of the ''largest'' region—i.e., the region for which the absolute value of the first Dirichlet Laplacian eigenvalue would be the smallest under the absence of channels (Figs. 5, 8, and 10).

ACKNOWLEDGMENTS

This work was supported in part by KBN Grant No. 2P03B00923 (2002-2004) and KBN Grant No. 5P03B01121.

APPENDIX

We prove that the entropy production σ [see Eqs. (32) and (33)] is a strictly monotonically decreasing function of time (the H theorem), except for the stationary state, where σ is constant and minimized:

$$\begin{aligned}\frac{\mathrm{d}\sigma}{\mathrm{d}t}&=\frac{\mathrm{d}}{\mathrm{d}t}\left(\frac{-2K\int_V p\Delta p\,\mathrm{d}V}{\int_V p^2\,\mathrm{d}V}\right)\\ &=\frac{2K}{\left(\int_V p^2\,\mathrm{d}V\right)^2}\left[2\int_V p\Delta p\,\mathrm{d}V\int_V p\frac{\partial p}{\partial t}\mathrm{d}V\right.\\ &\quad\left.-\left(\int_V\frac{\partial p}{\partial t}\Delta p\,\mathrm{d}V+\int_V p\Delta\frac{\partial p}{\partial t}\mathrm{d}V\right)\int_V p^2\,\mathrm{d}V\right]\\ &=\frac{2K^2}{\left(\int_V p^2\ \mathrm{d}V\right)^2}\left[2\left(\int_V p\Delta p\,\mathrm{d}V\right)^2-\int_V p^2\,\mathrm{d}V\right.\\ &\quad\left.\times\int_V(\Delta p)^2\,\mathrm{d}V-\int_V p^2\,\mathrm{d}V\int_V p\Delta(\Delta p)\,\mathrm{d}V\right].\end{aligned}$$

The last of the above passages was obtained after substituting the PDF time derivative by the expression given in Eq. (10). From the Green theorem we get the following identity:

$$\begin{aligned}\int_V p\Delta(\Delta p)\,\mathrm{d}V&=\int_V(\Delta p)^2\,\mathrm{d}V+\oint_{\partial V}p\nabla\Delta p\cdot\mathrm{d}\mathbf{S}\\ &\quad-\oint_{\partial V}\Delta p\nabla p\cdot\mathrm{d}\mathbf{S},\end{aligned}$$

where the surface integrals are both equal to zero, in accordance with Eq. (7). Finally,

$$\frac{\mathrm{d}\sigma}{\mathrm{d}t}=\left(\frac{2K}{\int_V p^2\,\mathrm{d}V}\right)^2\times\underbrace{\left[\left(\int_V p\Delta p\,\mathrm{d}V\right)^2-\left(\int_V p^2\,\mathrm{d}V\right)\left(\int_V(\Delta p)^2\,\mathrm{d}V\right)\right]}_{\text{further estimated as } H}$$

In the reciprocal space, with definitions in Eqs. (14) and (16), the term marked as H takes the following form:

$$\begin{aligned}H&=\left(\sum_i c_i^2\lambda_i\right)^2-\left(\sum_i c_i^2\right)\left(\sum_i c_i^2\lambda_i^2\right)\\ &=\sum_i c_i^2\lambda_i\sum_j c_j^2\lambda_j-\sum_i c_i^2\sum_j c_j^2\lambda_j^2\\ &=\sum_{i,j} c_i^2c_j^2\lambda_i\lambda_j-\frac{1}{2}\left(\sum_{i,j} c_i^2c_j^2\lambda_j^2+\sum_{i,j} c_i^2c_j^2\lambda_i^2\right)\\ &=-\frac{1}{2}\sum_{i,j} c_i^2c_j^2(\lambda_i-\lambda_j)^2.\end{aligned}$$

Except for the stationary state, the expression above is always negative [we use fact that $\forall t c_1 \neq 0$; see Eq. (18) and the text below it]. Thus the entropy production σ is a strictly monotonically decreasing function of time (or constant, but only in the stationary state), and in the limit of $t \to \infty$ it approaches the value given by Eq. (34) (which is because the evolution of the system approaches the stationary state; see [25]).

[1] S.R. Groot and P. Mazur, *Non-equilibrium Thermodynamics* (Dover, New York, 1984).
[2] L. Rondoni and E.G.D. Cohen, Physica D **168**, 341 (2002).
[3] D.J. Evans and A. Baranyai, Phys. Rev. Lett. **67**, 2597 (1991).
[4] W. Breymann, T. Tel, and J. Vollmer, Phys. Rev. Lett. **77**, 2945 (1996).
[5] J. Volmer, T. Tel, and W. Breymann, Phys. Rev. Lett. **79**, 2759 (1997).
[6] P. Gaspard and G. Nicolis, Phys. Rev. Lett. **65**, 1693 (1990).
[7] J. Vollmer, L. Matyas, and T. Tel, J. Stat. Phys. **109**, 875 (2002).
[8] J.A.S. Lima, R. Silva, and A.R. Plastino, Phys. Rev. Lett. **86**, 2938 (2001).
[9] U.M.S. Costa, M.L. Lyra, A.R. Plastino, and C. Tsallis, Phys. Rev. E **56**, 245 (1997).
[10] C. Tsallis and D.J. Bukman, Phys. Rev. E **54**, R2197 (1996).
[11] A.K. Rajagopal, Phys. Rev. Lett. **76**, 3469 (1996).
[12] C. Anteneodo and C. Tsallis, Phys. Rev. Lett. **80**, 5313 (1998).
[13] A.R.R. Papa and C. Tsallis, Phys. Rev. E **57**, 3923 (1998).
[14] C. Essex, C. Schulzky, A. Franz, and K.H. Hoffmann, Physica A **284**, 299 (2000).
[15] M.L. Lyra and C. Tsallis, Phys. Rev. Lett. **80**, 53 (1998).
[16] S. Abe, Physica A **300**, 417 (2001).
[17] E.K. Lenzi, R.S. Mendes, and L.R. Silva, Physica A **280**, 337 (2000).
[18] R.S. Johal, Phys. Rev. E **58**, 4147 (1998).
[19] A.R. Plastino and A. Plastino, Physica A **258**, 429 (1998).
[20] T.D. Frank and A. Daffertshofer, Physica A **272**, 497 (1999).
[21] T.D. Frank and A. Daffertshofer, Physica A **285**, 351 (2000).
[22] K. Burdzy, R. Hołyst, D. Ingerman, and P. March, J. Phys. A **29**, 2633 (1996).
[23] K. Burdzy, R. Hołyst, and P. March, Commun. Math. Phys. **214**, 679 (2000).
[24] R. Courant and D. Hilbert, *Method of Mathematical Physics* (Interscience, New York, 1953), Vol. I, Chap. VI, Sec. 6, p. 451.
[25] S. Port and C. Stone, *Brownian Motion and Classical Potential Theory* (Academic, New York, 1978), Chap. IV, Sec. 7, pp. 121–127.